

Stable Complete Water Splitting by Covalent Triazine-based Framework CTF-0

Dan Kong,^[a, d] Jijia Xie,^[a] Zhengxiao Guo,^[b] Dongyuan Yang,^{*,[c]} and Junwang Tang^{*,[a]}

D. K and J. T thank the financial support from UK EPSRC (EP/N009533/1), Royal Society-Newton Advanced Fellowship grant (NA170422) and the Leverhulme Trust (RPG-2017-122). D. K is also grateful for financial support by the UCL Engineering Dean's Prize and the Chinese Scholarship Council (CSC) for a PhD studentship.

Photocatalytic water splitting into H₂ and O₂ simultaneously is a highly promising pathway towards clean and renewable energy supply for the future.^[1] The ultimate goal to this end is to develop an efficient, low cost and stable photocatalyst available for overall water splitting without using sacrificial agents and external bias.^[2] However, it still remains challenging to identify a single photocatalyst material, which processes (i) a sufficiently narrow bandgap (<3 eV) to harness visible photons,^[3] (ii) suitable band-edge potentials for overall water splitting (*i.e.*, simultaneous production of H₂ and O₂),^[4] (iii) a high level of stability against photocorrosion and (iv) relatively low cost.^[5] In this regard, various inorganic semiconductors have been explored for overall water splitting,^[6] with few successful cases, but it is possible when composed with other materials,^[2d,7] such as the very recent report on Rh/Cr₂O₃-modified Ta₃N₅/KTaO₃ (with a solar to fuel conversion efficiency of 0.014%), which also indicate the significance of cocatalysts.^[8]

It is encouraging to witness recent growing interest in conjugated-based frameworks on the application of photocatalysis.^[1b,9] CTFs were recently reported for half reactions of water splitting in the presence of relevant sacrificial reagents,^[10] indicating that such CTFs could be good candidates for pure water splitting. CTFs are characterised by high porosities paired with exceptional inertness and high thermal stability owing to their graphite-like composition and aromatic carbon-carbon and carbon-nitrogen linkages.^[11] The CTFs could be impregnated with already formed metal nanoparticles, yielding hybrid materials with well-dispersed nanoparticles immobilized on the CTF support. Metal-modified CTFs exhibit superior activity, stability and, hence, recyclability in oxidation reactions as compared to other carbon supports modified with smaller amounts of nitrogen.^[11–12] Moreover, the presence of stoichiometric and well-defined nitrogen sites in the triazine frameworks has recently shown to be selectively sited by the catalytically active metal ions strong nitrogen-metal interactions, which renders CTFs promising catalysts and catalyst supports.^[12b,13] Among CTFs, CTF-0 features higher nitrogen content than the other members of the CTF family.^[14] The framework structure is shown in Scheme S1. Taking into account the excellent performance of CTF-0 for both water oxidation and reduction reactions,^[15] it is highly possible to achieve pure water splitting over this single photocatalyst. However, such one-step overall water splitting by CTF-0 photocatalysts without any sacrificial agent has not been reported so far. The optimised CTF-0 photocatalysts with cocatalysts Pt and CoO_x indicate an efficient way for solar H₂ production from water.

The CTF-0 photocatalyst was synthesized by an ionothermal method. Following the successful fabrication of crystalline polymer, different amount of Pt and Co₃O₄ were loaded on CTF-0 by the photodeposition method and impregnation method, separately (details are in the SI). Both X-ray powder diffraction (XRD) and ¹³C solid-state nuclear magnetic resonance (ssNMR) spectra of pure CTF-0 and cocatalysts decorated samples shown the typical patterns of CTF-0 as presented in Figure 1. Two distinct peaks at 15° and 26° could be distinguished in the XRD spectra in Figure 1(a), indicating some degree of extended order of the sample, while the intensity and width of the peaks could be influenced by the monomer to ZnCl₂ ratio and reaction time and temperature.^[14] Even these peaks were too broad to give a conclusive picture on the atomistic structure of CTF-0, the low-angle peak could be interpreted as the in-plane reflection (100) and the diffraction peak at ~26° could be attributed to an inter-layer spacing between stacked sheets of CTF-0 (3.35 Å). There are some small peaks at 19°, 32°, 37°

[a] Dr. D. Kong, Dr. J. Xie, Prof. J. Tang
Department of Chemical Engineering
University College London
Torrington Place, London, WC1E 7JE (UK)
E-mail: junwang.tang@ucl.ac.uk

[b] Prof. Z. Guo
Department of Chemistry, Faculty of Science
The University of Hong Kong
Pokfulam Road, Hong Kong (P. R. China)

[c] Dr. D. Yang
Xi'an Clean Energy(chemical) Research Institute
Shaanxi Yanchang Petroleum (Group) Corp. Ltd & Dalian Institute of
Chemical Physics
61 Tangyan St, Xi'an, 710075 (P. R. China)
E-mail: yangdongyuan@sxycpc.oa

[d] Dr. D. Kong
Current address:
School of Chemical Engineering
Aalto University
Kemistintie 1, Espoo, 02150 (Finland)

Supporting information for this article is available on the WWW under
<https://doi.org/10.1002/cctc.201902396>

© 2020 The Authors. Published by Wiley-VCH Verlag GmbH & Co. KGaA. This is an open access article under the terms of the Creative Commons Attribution License, which permits use, distribution and reproduction in any medium, provided the original work is properly cited.

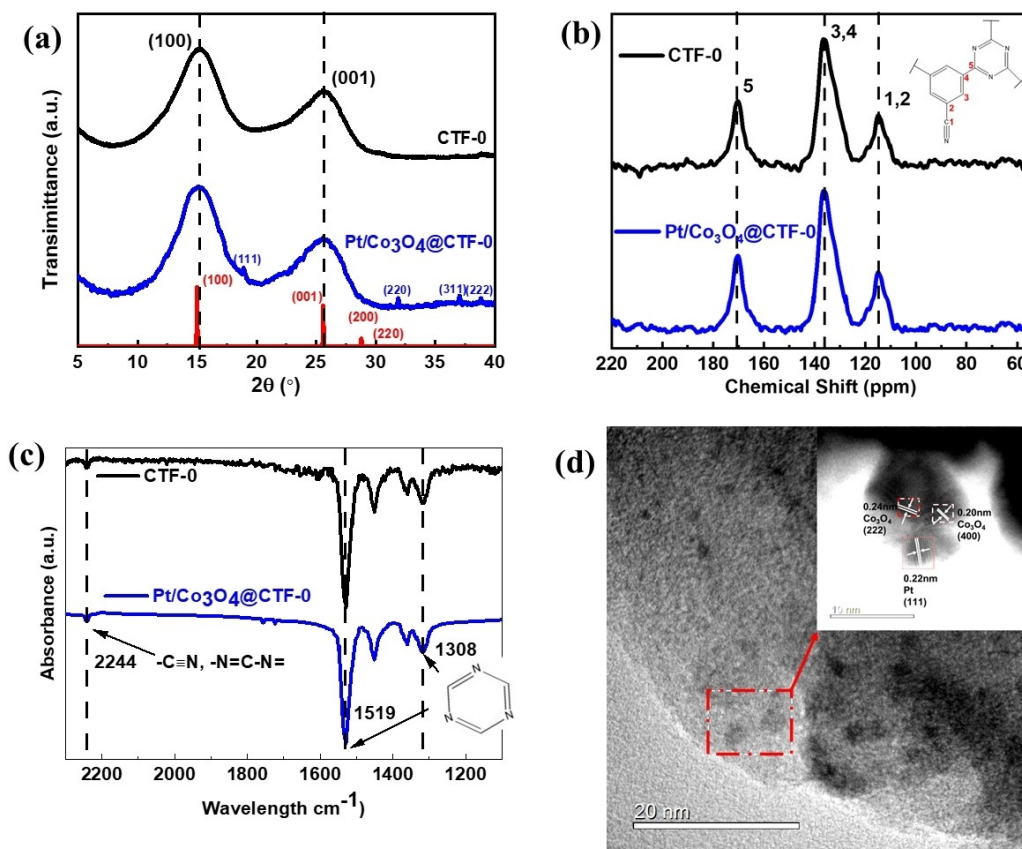


Figure 1. (a) XRD patterns and calculated based on AA-stacking motif, (b) ^{13}C CP-MAS ssNMR spectra, (c) FTIR spectra of CTF-0 and Pt/Co₃O₄@CTF-0, and (d) TEM and HRTEM (insert) images of 6 wt% Co₃O₄ and 3 wt% Pt-deposited CTF-0.

and 39° in the Pt/Co₃O₄@CTF-0 sample, which do not exist in the CTF-0 sample and can be indexed to cobalt oxide particles.^[16] The ^{13}C CP-MAS ssNMR shows the three distinct peaks in Figure 1(b), the peak at 171 ppm can be assigned to the carbon atoms in the triazine units, the peak at 138 ppm to the carbon atoms in the benzene units, and the peak at 117 ppm to the unreacted cyano groups and the neighbouring carbon in the benzene rings. Furthermore, only one peak at -121 ppm in both ^{15}N ssNMR spectra was observed in Figure S1, which is assigned to the triazine moiety,^[11] proving the stability of the materials before and after cocatalyst decoration. The FTIR spectra in Figure 1c show the vibrational fingerprints of triazine rings at 1308 and 1519 cm^{-1} . The small peak of CTF-0 at 2244 cm^{-1} belongs to the cyano groups, which has the similar height after decorating the cocatalysts on the photocatalysts. In a short summary, all these characterizations illustrate the chemical structure of the frameworks keep stable after cocatalysts decoration.

To further examine the existence of the cocatalysts on the surface of the photocatalysts, X-ray photoelectron spectroscopy (XPS) measurements were conducted. Obviously, the XPS survey of the CTF-0 samples only shows the peaks of carbon and nitrogen elements in Figure S2, while the sample of Pt/Co₃O₄@CTF-0 s also has the peaks of cobalt and platinum, e.g. around 790 (Co 2p) and (Pt 4f) 70 eV, respectively. A small

amount of oxygen was also detected from the survey spectra, which was from the cocatalysts cobalt oxide. For the cocatalysts Co₃O₄, the high-resolution XPS spectrum of Co 2p shows two major peaks with binding energies of 779.5 and 794.8 eV, corresponding to Co 2p_{3/2} and Co 2p_{1/2}, respectively (Figure S3). The energy difference between the Co 2p_{3/2} and Co 2p_{1/2} splitting is around 15 eV, which indicates the existence of Co²⁺ and Co³⁺ and likely corresponds to the existence of Co₃O₄.^[17] The two small peaks at 784.9 and 800.2 eV are typical Co²⁺ shakeup satellite peaks. Correspondingly, the deconvoluted XPS spectra for O 1s displays two types of contributions for oxygen species shown in Figure S4. The one peak at 529.7 eV is dominant and is corresponding to the cobalt oxides, and the other one at 531.1 eV indicates the presence of –OH species on the surfaces of cobalt oxide cocatalysts.^[17b] To investigate the electronic structures of Pt, the Pt 4f XPS spectra were measured in Figure S5. The Pt 4f spectrum can be deconvoluted into two pairs of doublets. The deconvoluted peaks at 71.3 and 74.7 eV are ascribed to the 4f_{7/2} and 4f_{5/2} peaks of Pt metal, respectively.^[18] The set of peaks at 72.7 and 76.1 eV are assigned to the 4f_{7/2} and 4f_{5/2} peaks of Pt²⁺ (PtO or Pt(OH)₂), respectively. A comparison of the relative areas of the integrated intensity of the Pt⁰ and Pt²⁺ peaks in Figure S5 (the area ratio is 2.2:1) indicates that most of the Pt elements exist as Pt⁰ in the cocatalysts, which should help H₂ evolution in the following

overall water splitting as reported.^[19] Moreover, TEM observation was carried out and shown in Figure 1(d) to investigate the architecture of the cocatalysts on the surface of the samples. It can be seen that the cocatalyst particles are dispersed on the photocatalysts. The high resolution TEM image shows clear lattice fringes in the sample (Figure S6). The lattice spacing of Pt is 0.22 nm next to the d(111) and (400) crystal planes of cubic Co₃O₄. The TEM analyses together with the XPS results indicate the Pt and Co₃O₄ nanoparticles were decorated on the surface of CTF-0 successfully.

The half reactions of overall water splitting for H₂ and O₂ evolution were first tested as shown in Figure 2 (a) and (b), respectively. For comparison, pure CTF-0 was served as a reference. Obviously, 0.01 g CTF-0 could produce H₂ of 22.62 μmol h⁻¹ with Pt as a cocatalysts stably in the presence of TEOA as the sacrificial agent, more than 200 folds enhancement and extremely higher than that without Pt under full arc irradiation (Figure 2(a)). On the other side, Co₃O₄ decorated CTF-0 have much higher initial O₂ evolution rate, namely 3.65 μmol in the first hour, twice higher than pure CTF-0, more than 36 times of pure Co₃O₄ (Figure 2(b)). Following these successful half reactions, the decoration of both Pt and Co₃O₄ on CTF-0 has been explored to realize the overall water splitting into H₂ and O₂ and the results are shown in Figure 2 (c) and (d).

The pure CTF-0 (blank) sample exhibits no detectable activity toward overall water splitting. However, hydrogen and oxygen gases were detected when co-deposited Pt and Co₃O₄ on the CTF-0 surface. This result demonstrates that the loading of cocatalysts is a critical step to induce the pure water splitting reaction. The stoichiometric ratio of hydrogen and oxygen equal to 2:1 was achieved when both Pt and Co₃O₄ cocatalysts were loaded on the surface of the photocatalysts, interpreting that the evolved O₂ is mostly originated from water oxidation. It is also suggested that the photogenerated electrons and holes are well separated and equally consumed by the water splitting reaction with the highest efficiency when 6 wt% Co₃O₄ and 3 wt % Pt were decorated on the surface of CTF-0 photocatalysts. A long-time course of the simultaneous evolution of H₂ and O₂ for the overall water splitting on 3 wt% Pt and 6 wt% Co₃O₄ deposited CTF-0 without any sacrificial agent was mentioned and is shown in Figure 2 (d). H₂ and O₂ evolution are observed only after turning on the light, confirming a photoactive response. The both gas evolutions show constant rates with an expected molar ratio of 2:1 for H₂/O₂. Moreover, the photocatalytic activity displays no noticeable reduction in an 18 h-reaction, and the FTIR spectra of Pt/Co₃O₄@CTF-0 before and after the photocatalysis during the prolonged operation remain unchanged as shown in Figure S7. All the above confirm the

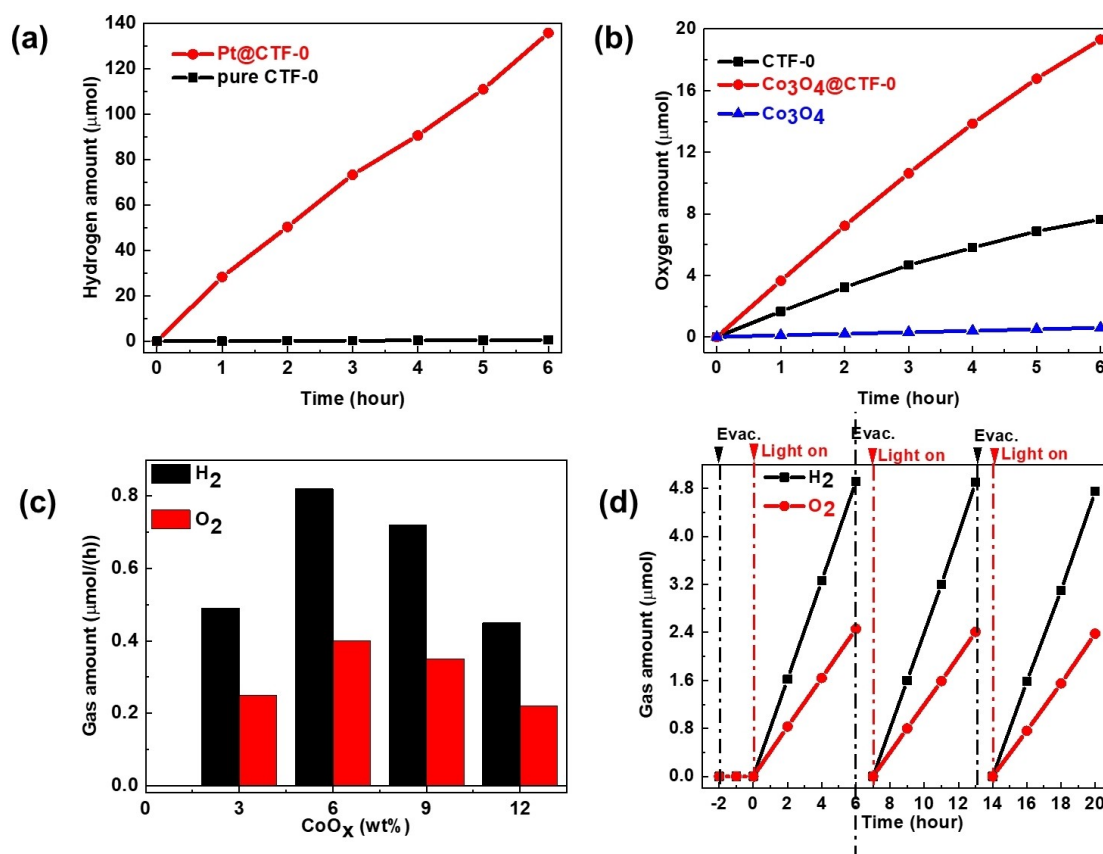


Figure 2. (a) H₂ half reaction by pure and 3 wt% Pt-deposited CTF-0 with TEOA as the sacrificial agent, (b) O₂ half reaction by pure and 6 wt% Co₃O₄-deposited CTF-0 with AgNO₃ as the sacrificial agent, (c) photocatalytic overall water splitting of different amounts of Co-loaded on CTF-0 with 3 wt% Pt as co-catalysts except for the blank one, (d) cyclic runs of H₂ and O₂ production from pure water by 6 wt% Co₃O₄ and 3 wt% Pt-deposited CTF-0. All the experiments were under full arc irradiation of a 300 W Xe lamp and 10 mg photocatalysts were used.

stability of the photocatalysts and the solar to fuel conversion efficiency was measured to be about 0.028%, which is moderate while higher than the recently reported inorganic system (Rh/Cr₂O₃-modified Ta₃N₅/KTAO₃).^[5] These results suggest that the suitable amount of Pt and Co species on the surface of CTF-0 is of crucial significance for the photocatalytic overall water splitting, resulting into a turn over number of 958 with respect to Pt and 593 with respect to Co₃O₄ assuming all powders of Pt and Co₃O₄ are active sites. This clearly underestimates the performance of the photocatalyst to some extent.

Efficient optical absorption and charge separation are of great importance for a photocatalytic reaction. In the UV-vis spectra, the typical band edge of the CTF-0 photocatalyst is observed at around 400 nm, as shown in Figure S8. Correspondingly, the bandgap of CTF-0 is calculated as 3.0 eV, observed from the Tauc plots of the UV-vis absorption data. After coupling with Pt particles on CTF-0, the absorption edge has no discernible change, indicating that the introduction of Pt cocatalysts does not affect the band structure. However, after loading cobalt oxide cocatalysts into Co₃O₄@CTF-0, there is an additional absorption edge at ca. 430 nm, and the corresponding bandgap is ca. 2.9 eV. For the absorption edge at 480 nm, this absorption ($\lambda < 500$ nm) were referred to ligand-metal charge transfer events O(II)→Co(II).^[20] As a result of decoration

of both Pt and Co₃O₄ on the surface of CTF-0, the UV-vis light absorption shows two sharp absorption edges at 430 nm and 480 nm and the corresponding band gaps were 2.9 and 2.6 eV. So, the two-bandgap absorption should be attributed to bandgap absorption of CTF-0 and Co₃O₄.

For the investigation of the transfer of photoexcited electron-hole pairs, photoelectrochemical analysis was performed on the CTF-0 and Pt/Co₃O₄@CTF-0 excited by the simulated solar light. The increase of photocurrent was confirmed by transient photocurrent response as shown in Figure 3 (a), The Pt/Co₃O₄@CTF-0 exhibits a higher photocurrent than the pure CTF-0, which likely indicates the more efficient separation and transmission of the photogenerated carriers. The impedance arc radius of Pt/Co₃O₄@CTF-0 is much smaller than pure CTF-0 (Figure 3 (b)), indicating the better electrical conductivity, which would facilitate the migration of the photoexcited carriers and therefore, enhancing the photocatalytic efficiency. Figure S9 presents the offset of the sample in the binding energies of the valence electrons, i.e. +2.1 eV. In a typical XPS measurement, the binding energy of an electron represents the energy that the electron requires to occupy the Fermi level of the XPS analyser. The work function of the XPS analyser is ca. 4 (vs. vacuum) and -0.4 eV (vs. RHE at pH=0).^[21] Thus, the valence band positions of vs RHE at pH=0 can be

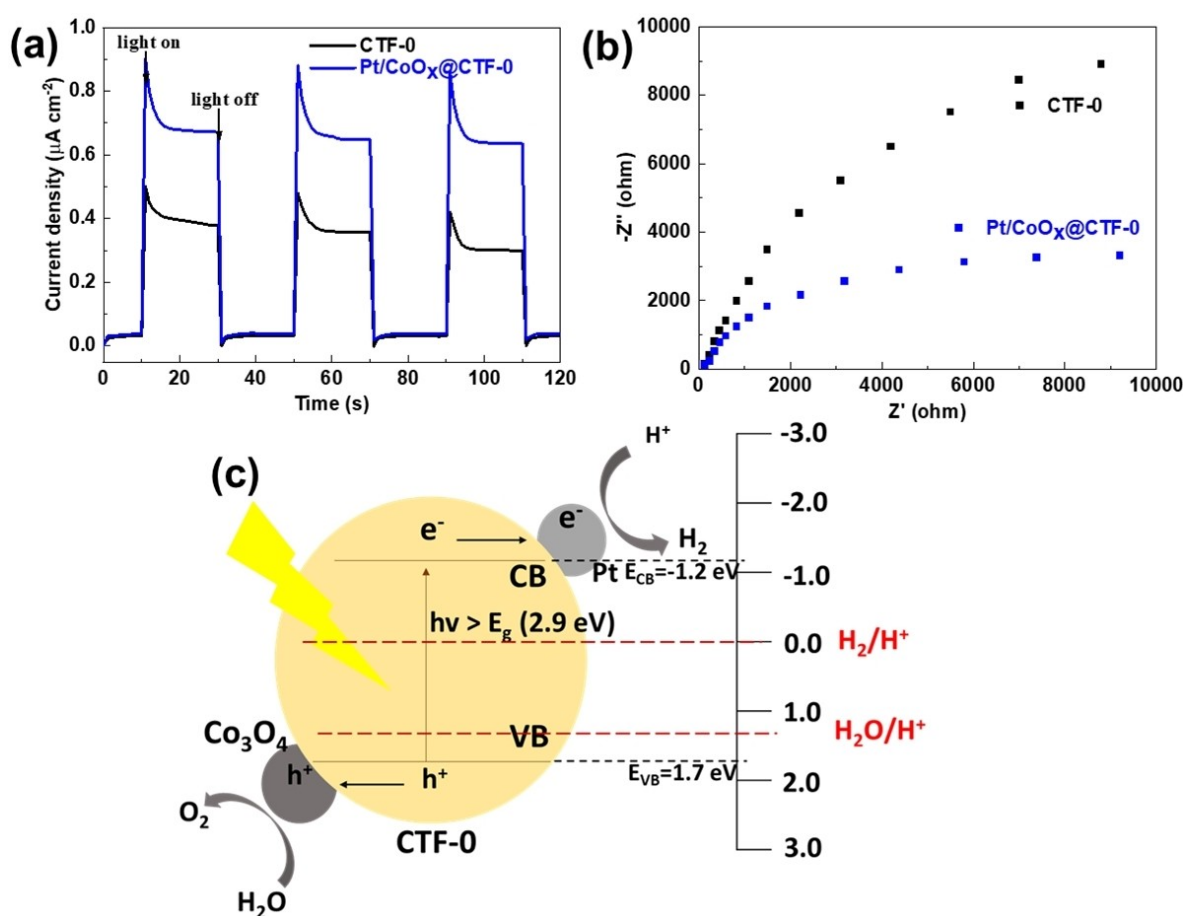


Figure 3. (a) transient photocurrent response, (b) electrochemical impedance spectroscopy Nyquist plots of CTF-0 and Pt/Co₃O₄@CTF-0 in 0.1 M Na₂SO₄ with 0.4 V bias versus Ag/AgCl and pH = 6.5, and (c) proposed schematic of the photocatalytic overall water splitting reaction mechanism on Pt/Co₃O₄@CTF-0.

estimated at +1.7 eV. Given the band gap obtained from the Tauc plots in Figure S8 and the XPS electron spectra, the conduction band position was deduced as -1.2 eV. Therefore, the band positions of Pt/Co₃O₄@CTF-0 are shown in Figure 3(c). In light of the above results and analysis, a schematic illustration of the reaction mechanism on the Pt/Co₃O₄@CTF-0 was proposed in Figure 3 (c). Firstly, the electrons are excited from the valence band (VB) of CTF-0 to the respective conduction band (CB) under light irradiation. Next, the generated electrons and holes transfer to the Pt and Co₃O₄ cocatalysts as evidenced by photoelectrochemical and impedance scans. These cocatalysts with separated charges can catalyse proton reduction ($2e^- + 2H^+ \rightarrow H_2$) and water oxidation ($2H_2O + 4h^+ \rightarrow O_2 + 4H^+$) for the overall water splitting, respectively.^[22] At this point, decorating cocatalysts on CTF-0 can increase the charge carrier separation and transfer, and more importantly realise the photocatalytic activity of the overall water splitting.

In summary, it is demonstrated, for the first time, that photocatalytic overall water splitting over a single CTF-0 photocatalyst has been achieved by loading both Pt and Co₃O₄ as cocatalysts. The photocatalytic activity of the cocatalyst-modified CTF-0 was improved greatly in each half reaction of water splitting. A hydrogen production rate of 2262 $\mu\text{mol g}^{-1} \text{h}^{-1}$ and an initial oxygen evolution level of 365 $\mu\text{mol g}^{-1}$ were achieved in the water reduction and oxidation reaction, respectively. The stoichiometric ratio of H₂/O₂=2:1 was obtained by adjusting the levels of Co₃O₄ and Pt cocatalysts; and the optimum is 6 wt % Co₃O₄ and 3 wt% Pt, leading to 82 $\mu\text{mol g}^{-1} \text{h}^{-1}$ H₂ and 40 $\mu\text{mol g}^{-1} \text{h}^{-1}$ O₂ produced in 18 hours, resulting into a turn over number of 958 over Pt and 593 over Co₃O₄. Based on the light absorption and photoelectrochemical measurements, it is found that loading both Pt and Co₃O₄ is essential for the overall water splitting of CTF-0, which offers more active sites, and accelerates the transfer of photogenerated charges. The one-step approach of water splitting on CTF-0 provides new insight into the artificial photocatalysis and represents a promising route for further practical applications.

Conflict of Interest

The authors declare no conflict of interest.

Keywords: covalent triazine framework-0 · overall water splitting · Pt cocatalyst · Co₃O₄ cocatalyst · hydrogen fuel

[1] a) Y. Wang, H. Suzuki, J. Xie, O. Tomita, D. J. Martin, M. Higashi, D. Kong, R. Abe, J. Tang, *Chem. Rev.* **2018**, *118*(100), 5201–5241; b) J. Xie, S. Shevlin, Q. Ruan, S. Moniz, Y. Liu, X. Liu, Y. Li, C. C. Lau, Z. X. Guo, J. Tang, *Energy Environ. Sci.* **2018**, *11*(6), 1617–1624.

- [2] a) J. Suntivich, K. J. May, H. A. Gasteiger, J. B. Goodenough, Y. Shao-Horn, *Science* **2011**, *334*, 1383–1385; b) M. Hara, T. Kondo, M. Komoda, S. Ikeda, J. N. Kondo, K. Domen, M. Hara, K. Shinohara, A. Tanaka, *Chem. Commun.* **1998**, 357–358; c) G. Zhang, Z.-A. Lan, L. Lin, S. Lin, X. Wang, *Chem. Sci.* **2016**, *7*, 3062–3066; d) J. Liu, J. Ke, Y. Li, B. Liu, L. Wang, H. Xiao, S. Wang, *Appl. Catal. B* **2018**, *236*, 396–403; e) L. Wang, Y. Wan, Y. Ding, S. Wu, Y. Zhang, X. Zhang, G. Zhang, Y. Xiong, X. Wu, J. Yang, H. Xu, *Adv. Mater.* **2017**, *29*, 1702428.
- [3] R. Li, Y. Weng, X. Zhou, X. Wang, Y. Mi, R. Chong, H. Han, C. Li, *Energy Environ. Sci.* **2015**, *8*, 2377–2382.
- [4] X. Wang, Q. Xu, M. Li, S. Shen, X. Wang, Y. Wang, Z. Feng, J. Shi, H. Han, C. Li, *Angew. Chem. Int. Ed.* **2012**, *51*, 13089–13092.
- [5] a) K. Maeda, *J. Photochem. Photobiol. A* **2011**, *12*, 237–268; b) K. Maeda, K. Teramura, T. Takata, M. Hara, N. Saito, K. Toda, Y. Inoue, H. Kobayashi, K. Domen, *J. Phys. Chem. B* **2005**, *109*, 20504–20510.
- [6] a) C. T. K. Thaminimulla, T. Takata, M. Hara, J. N. Kondo, K. Domen, *J. Catal.* **2000**, *196*, 362–365; b) Z. Zou, J. Ye, K. Sayama, H. Arakawa, *Nature* **2001**, *414*, 625–627.
- [7] C. Pan, T. Takata, M. Nakabayashi, T. Matsumoto, N. Shibata, Y. Ikuhara, K. Domen, *Angew. Chem. Int. Ed.* **2015**, *54*, 2955–2959.
- [8] a) K. Kato, K. Asakura, A. Kudo, *J. Am. Chem. Soc.* **2003**, *125*, 3082–3089; b) K. Maeda, M. Higashi, D. Lu, R. Abe, K. Domen, *J. Am. Chem. Soc.* **2010**, *132*, 5858–5868.
- [9] a) W. Liu, L. Cao, W. Cheng, Y. Cao, X. Liu, W. Zhang, X. Mou, L. Jin, X. Zheng, W. Che, Q. Liu, T. Yao, S. Wei, *Angew. Chem. Int. Ed.* **2017**, *56*, 9312–9317; b) L. Wang, X. Zheng, L. Chen, Y. Xiong, H. Xu, *Angew. Chem.* **2018**, *57*, 3454–3458; c) W. Che, W. Cheng, T. Yao, F. Tang, W. Liu, H. Su, Y. Huang, Q. Liu, J. Liu, F. Hu, Z. Pan, Z. Sun, S. Wei, *J. Am. Chem. Soc.* **2017**, *139*, 3021–3026.
- [10] a) X. Jiang, P. Wang, J. Zhao, *J. Mater. Chem. A* **2015**, *3*, 7750–7758; b) J. Bi, W. Fang, L. Li, J. Wang, S. Liang, Y. He, M. Liu, L. Wu, *Macromol. Rapid Commun.* **2015**, *36*, 1799–1805; c) L. Li, W. Fang, P. Zhang, J. Bi, Y. He, J. Wang, W. Su, *J. Mater. Chem. A* **2016**, *4*, 12402–12406.
- [11] S. Hug, M. E. Tauchert, S. Li, U. E. Pachmayr, B. V. Lotsch, *J. Mater. Chem.* **2012**, *22*, 13956–13964.
- [12] a) C. E. Chan-Thaw, A. Villa, P. Katekomol, D. Su, A. Thomas, L. Prati, *Nano Lett.* **2010**, *10*, 537–541; b) C. E. Chan-Thaw, A. Villa, L. Prati, A. Thomas, *Chem. Eur. J.* **2011**, *17*, 1052–1057.
- [13] a) C. E. Chan-Thaw, A. Villa, P. Katekomol, D. Su, A. Thomas, L. Prati, *Nano Lett.* **2010**, *10*, 537–541; b) R. Palkovits, M. Antonietti, P. Kuhn, A. Thomas, F. Schüth, *Angew. Chem. Int. Ed.* **2009**, *48*, 6909–6912.
- [14] P. Katekomol, J. Roeser, M. Bojdy, J. Weber, A. Thomas, *Chem. Mater.* **2013**, *25*, 1542–1548.
- [15] D. Kong, X. Han, J. Xie, Q. Ruan, C. D. Windle, S. Gadipelli, K. Shen, Z. Bai, Z. Guo, J. Tang, *ACS Catal.* **2019**.
- [16] X. Chen, J. P. Cheng, Q. L. Shou, F. Liu, X. B. Zhang, *CrystEngComm* **2012**, *14*, 1271–1276.
- [17] a) J. Yang, H. Liu, W. N. Martens, R. L. Frost, *J. Phys. Chem. C* **2010**, *114*, 111–119; b) R. R. Salunkhe, J. Tang, Y. Kamachi, T. Nakato, J. H. Kim, Y. Yamauchi, *ACS Nano* **2015**, *9*, 6288–6296.
- [18] a) M. A. Matin, E. Lee, H. Kim, W.-S. Yoon, Y.-U. Kwon, *J. Mater. Chem. A* **2015**, *3*, 17154–17164; b) H. Xu, L.-X. Ding, C.-L. Liang, Y.-X. Tong, G.-R. Li, *NPG Asia Mater.* **2013**, *5*, e69–e69.
- [19] X. Wang, K. Maeda, A. Thomas, K. Takane, G. Xin, J. M. Carlsson, K. Domen, M. Antonietti, *Nat. Mater.* **2008**, *8*, 76.
- [20] D. Barreca, C. Massignan, S. Daolio, M. Fabrizio, C. Piccirillo, L. Armelao, E. J. C. o M Tondello, *Chem. Mater.* **2001**, *13*, 588–593.
- [21] C. G. Van de Walle, *Physica B + C* **2006**, *376*, 1–6.
- [22] D. Kong, Y. Zheng, M. Kobielski, Y. Wang, Z. Bai, W. Macyk, X. Wang, J. Tang, *Mater. Today* **2018**, *21*, 897–924.

Manuscript received: December 29, 2019
 Revised manuscript received: February 21, 2020
 Accepted manuscript online: February 24, 2020
 Version of record online: March 26, 2020